Advances and Applications in Mathematical Sciences
Volume 23, Issue 3, January 2024, Pages 153-181

ARITHMETICAL SCHEME FOR SOLVING EXOTHERMIC REACTIONS MODEL WITH A CONSTANT HEAT SOURCE IN A POROUS MEDIUM PROBLEMS BY THE OPERATIONAL MATRIX BASED ON FIBONACCI WAVELETS

S. C. SHIRALASHETTI[1*], E. HARISHKUMAR[2] and S. I. HANAJI[3]

[1,2]Department of Mathematics
Karnatak University, Dharwad-580003
Karnataka, India
E-mail: eharishkumar91@gmail.com

[3]Department of Mathematics
Dr. M. S. Sheshgiri College of Engineering and Technology
Udyambag, Belagavi-590008, Karnataka, India
E-mail: savitahanaji@gmail.com

Abstract

In this study, a precise and useful scheme is projected to solve the exothermic reaction model with a constant heat source in the porous medium. The model concentrates on the driving force to investigate the temperature profile. The governing equations of the problems with proper boundary conditions are reduced to nonlinear boundary value problems (BVPs) by applying similarity transformations. In the scheme, we simplify the governing BVPs using the Fibonacci wavelet operational matrix method. Using this scheme, the BVPs can be transformed into a set of algebraic equations and solved using Newton's iterative method. To check the efficiency of the proposed method, second-order linear and nonlinear boundary value problems having exact solutions are considered test problems and compared to the Haar wavelet operational matrix method (HWOMM) with exact solutions. Also, the obtained solutions are in great agreement and are more accurate compared to the HWOMM results.

2020 Mathematics Subject Classification: 34B05, 34B15, 76S05.
Keywords: Boundary value problems; Fibonacci wavelets; Operational matrices; Exothermic reaction; Heat source.
*Corresponding author; E-mail: scshiralashetti@kud.ac.in, shiralashettisc@gmail.com
Received November 22, 2022; Accepted January 31, 2023

1. Introduction

The exothermic reaction is a physical or chemical reaction that releases energy in the form of light and heat while also releasing net energy to its surroundings. It simply indicates that the energy required to initiate the reaction is less than the energy released afterward. In biological environments, energy is generated from chemical bonds. The energy is required when bonds are broken, the energy is released when bonds are created. There is bond energy for each sort of bond. By calculating bond energies, it is possible to forecast whether a chemical reaction will produce or consume heat. The heat is produced when more energy is expended to establish bonds than to break them, this reaction is called an exothermic reaction. A chemical reaction that necessitates the addition of energy is called an endothermic reaction. The capacity to break bonds is known as activation energy.

In recent years, convection has been increasingly popular in a variety of fields, to name a few, Geothermal energy extraction, Solar energy conversion, Groundwater contaminant transport, Oil reservoir simulation, Atmospheric dynamics, Energy extraction, Nuclear reactors, and Underground coal gasification. The Exothermic Reaction (ER) model is centered on a system where the driving force is due to temperature gradients applied at the system's boundary. The author Beck has investigated the critical Rayleigh number for a convective fluid flow in a rectangular box of saturated porous material [1-2]. Some researchers have discussed Rayleigh-Bernard-type convection [3-4]. They also studied how the ER model causes convective instabilities in a porous medium. S. Subramanian et al. have investigated the convective instabilities that are induced by ER in porous media [5]. Furthermore, Nopparat Pochai investigated the steady-state energy balance equation of the temperature profile in a conduction state with a constant heat source, the governing equation is solved using a finite difference technique [6]. A few studies have looked at two-and three-dimensional models of free convection among different types of porous mediums [7-9]. Recently, Fazle Mabood et al. have investigated that in porous media, exothermic reaction models can be used to solve problems using nonlinear ordinary differential equations [10]. The analytical solution of the ER model with a constant heat

source with a porous medium has been investigated by Ram Prakash Sharma et al. [11].

In recent years, the Fibonacci wavelet operational matrix method (FWOMM) is one of the most extensively used wavelet methods for computing numerical results for linear and nonlinear differential equations. Many researchers are discussed applying numerical methods to discover the results of linear and nonlinear boundary value problems with exact solutions [12-13]. Nowadays, in the literature, there are several types of wavelet-based techniques are available for solving nonlinear boundary value problems and controlling the challenges in numerical approaches for dealing with nonlinear boundary value problems [14-18]. The Fibonacci wavelet method is one of the most extensively used wavelet methods for computing numerical results of some classes of equations [19-21].

In this paper, the operational matrices based on the Fibonacci wavelet are established. These Fibonacci wavelet operational matrices are used to calculate the estimated solutions of the boundary value problems. This methodology moderates the boundary value problem to a set of algebraic equations by Fibonacci wavelet operational matrices. With the properties of the Fibonacci wavelets, we can abridge the boundary value problem. Furthermore, an innovative arithmetical scheme based on the Fibonacci wavelets is proposed for the numerical solution of characteristic nonlinear boundary value problems to investigate the heat transfer problem on the exothermic reactions model in the presence of a porous medium and constant heat source. The model concentrates on the driving force to investigate the temperature profile. The effects of several parameters are used such as ϕ, B and γ, have been discussed in detail and presented in terms of Tables and Figures.

2. Preliminaries of Fibonacci Wavelets

2.1 Fibonacci wavelets

2.1.1 Fibonacci polynomials

In general, the Fibonacci polynomials have been described in terms of recurrence relation as [20];

$$\widetilde{P}_m(z) = \begin{cases} 1, & m = 0, \\ z, & m = 1, \\ z\widetilde{P}_{m-1}(z) + \widetilde{P}_{m-2}(z), & m > 1. \end{cases} \tag{1}$$

And also can be introduced closed-form formulas,

$$\widetilde{P}_{m-1}(z) = \frac{\alpha^m - \beta^m}{\alpha - \beta}, \ (m \geq 1).$$

Where, α and β are the roots of the recursion's companion polynomial $x^2 - zx - 1$, and also the Fibonacci polynomials power form representation is as follows [20];

$$\widetilde{P}_m(z) = \sum_{i=0}^{\lfloor m/2 \rfloor} \binom{m-1}{i} z^{(m-2i)}, \ (m \geq 0). \tag{2}$$

The Fibonacci polynomials $\widetilde{P}_m(z)$ can alternatively be written in a matrix form, as seen below:

$\widetilde{P}(z) = UV(z)$, where $\widetilde{P}(z) = V(z)$ and U can be denoted as [19];

$$\widetilde{P}(z) = \begin{pmatrix} P_0(z) \\ P_1(z) \\ P_2(z) \\ P_3(z) \\ \vdots \end{pmatrix}, \ V(z) = \begin{pmatrix} 1 \\ z \\ z^2 \\ z^3 \\ \vdots \end{pmatrix}, \text{ and } U = \begin{pmatrix} 1 & 0 & 0 & 0 & 0 & 0 & 0 & \dots \\ 0 & 1 & 0 & 0 & 0 & 0 & 0 & \dots \\ 1 & 0 & 1 & 0 & 0 & 0 & 0 & \dots \\ 0 & 2 & 0 & 1 & 0 & 0 & 0 & \dots \\ 1 & 0 & 3 & 0 & 1 & 0 & 0 & \dots \\ 0 & 3 & 0 & 4 & 0 & 1 & 1 & \dots \\ \vdots & \vdots & \vdots & \vdots & \vdots & \vdots & \vdots & \ddots \end{pmatrix}. \tag{3}$$

The following satisfying properties of Fibonacci polynomials are as follows [19];

$$\int_0^{\eta} \widetilde{P}_m(s)ds = \frac{1}{m+1}\left[\widetilde{P}_{m+1}(z) + \widetilde{P}_{m-1}(z) - \widetilde{P}_{m+1}(0) + \widetilde{P}_{m-1}(0)\right], \tag{4}$$

$$\int_0^{l} \widetilde{P}_m(z)\widetilde{P}_n(z)d\eta = \sum_{i=0}^{\lfloor m/2 \rfloor} \sum_{j=0}^{\lfloor n/2 \rfloor} \binom{m-1}{i} \binom{m-j}{j} \frac{1}{m+n-2i-2j+1}. \tag{5}$$

2.1.2 Fibonacci wavelets and its approximation

Fibonacci wavelets are a type of compactly supported wavelet formed by Fibonacci polynomials over the interval $[0, 1]$. Generally, the Fibonacci wavelets can be represented in the interval $[0, 1)$ as [19].

$$\psi_{n,m}(z) = \begin{cases} \frac{2^{(k-1)/2}}{\sqrt{w_m}} \widetilde{P}_m(2^{k-1}z - n + 1), & \left(\frac{n-1}{2^{k-1}} \le z < \frac{n}{2^{k-1}}\right), \\ 0, & \text{otherwise.} \end{cases} \tag{6}$$

Where, k and n represent the level of resolution $k = 1, 2, \ldots$ with translation parameter $n = 1, 2, \ldots, 2^{k-1}$, and $\widetilde{P}_m(z)$ is the Fibonacci polynomial of degree m. With $w_m = \int_0^l \widetilde{P}_m^2(z)d\eta$ where $m = 0, 1, 2, \ldots, M-1$, the Fibonacci wavelets Equation (6) are also represented in the following way;

$$\psi_{n,m}(z) = \frac{2^{(k-1)/2}}{\sqrt{w_n}} \widetilde{P}_m(2^{(k-1)}z - n + 1)\chi_{I_{n,k}}(z), \tag{7}$$

Where, $\chi_{I_{n,k}}(z)$ is the specified characteristic function on $\left[\frac{n-1}{2^{k-1}}, \frac{n}{2^{k-1}}\right]$. For $k = 2$ and $M = 4$, the Fibonacci wavelet family consists,

$$\left.\begin{array}{l} \psi_{1,0}(z) = \sqrt{2}, \\ \psi_{1,1}(z) = 2\sqrt{6}z, \\ \psi_{1,2}(z) = \sqrt{(15/14)}\,(1 + 4z^2), \\ \psi_{1,3}(z) = \sqrt{(960/38)}\,(2z^3 + z), \end{array}\right\} \quad 0 \le z < \frac{1}{2},$$

$$\left.\begin{array}{l} \psi_{2,0}(z) = \sqrt{2}, \\ \psi_{2,1}(z) = \sqrt{6}\,(2z - 1), \\ \psi_{2,2}(z) = \sqrt{(30/7)}\,(2z^2 - 2z + 1), \\ \psi_{2,3}(z) = \sqrt{(480/304)}\,(8z^3 - 12z^2 + 10z - 3), \end{array}\right\} \quad \frac{1}{2} \le z < 1, \tag{8}$$

The Fibonacci wavelets may be used to extend any square-integrable function $f(z) \in L^2[0, 1]$ we have [18],

$$f(z) = \sum_{n=1}^{\infty} \sum_{m=0}^{\infty} a_{n,m} \psi_{n,m}(\eta), \tag{9}$$

By truncating the infinite series above, we obtain;

$$f(z) = \sum_{n=1}^{2^{k-1}} \sum_{m=0}^{M-1} a_{n,m} \psi_{n,m}(z) = a^T \Phi(\eta), \tag{10}$$

Where,

$$a_{n,m} = \langle f, \psi_{n,m} \rangle = \int_0^1 f(z) \psi_{n,m}(z) dz, \tag{11}$$

Equation (11) represents coefficients of the Fibonacci wavelet, and also the matrix equivalent of in Equation (10) is as follows [19];

$$f(z) = \psi(z) = a^T \Phi(z), \tag{12}$$

Where F is the discrete of continuous function, and a is a form of row vector can be written as;

$$a = [a_{1,0}, a_{1,1}, a_{1,2}, \ldots, a_{1,M-1}, a_{2,0}, a_{2,1}, \ldots, a_{2,M-1}, \ldots, a_{2^{k-1},0},$$

$$a_{2^{k-1},1}, \ldots, a_{2^{k-1},M-1}]^T, \tag{13}$$

and the matrix $\Phi(z)$ is $\hat{m} \times 1 (\hat{m} = 2^{k-1} M)$ given by

$$\Phi(z) = [\psi_{1,0}(z), \psi_{1,1}(z), \psi_{1,2}(z), \ldots, \psi_{1,M-1}(z), \psi_{2,0}(z), \psi_{2,1}(z), \ldots, \psi_{2,M-1}(z),$$

$$\ldots, \psi_{2^{k-1},0}(z), \psi_{2^{k-1},1}(z), \ldots, \psi_{2^{k-1},M-1}(z)]^T, \tag{14}$$

and from Equation (8) by using the collocation points given in Equation (15).

$$z_l = \frac{(l - 0.5)}{2^{k-1} M}, \; l = 1, 2, \ldots, 2^{k-1} M, \tag{15}$$

Generally, we can write the matrix form as follows;

$$\Phi_{\hat{m}\times\hat{m}} = \begin{bmatrix} \psi_1(z_1) & \psi_1(z_2) & \cdots & \psi_1(z_{2^{k-1}M}) \\ \psi_2(z_1) & \psi_2(z_2) & \vdots & \psi_1(z_{2^{k-1}M}) \\ \vdots & \vdots & \ddots & \vdots \\ \psi_{2^{k-1}M}(z_1) & \psi_{2^{k-1}M}(z_2) & \cdots & \psi_{2^{k-1}M}(z_{2^{k-1}M}) \end{bmatrix},$$

For instance, if $k = 2$ and $M = 4$, we can write the coefficients matrix of Fibonacci wavelets as follows;

$$\psi_{8\times8}(z_l) = \begin{bmatrix} \frac{239}{169} & \frac{239}{169} & \frac{239}{169} & \frac{239}{169} & 0 & 0 & 0 & 0 \\ \frac{94}{307} & \frac{203}{221} & \frac{173}{113} & \frac{688}{321} & 0 & 0 & 0 & 0 \\ \frac{41}{39} & \frac{183}{155} & \frac{95}{66} & \frac{53}{29} & 0 & 0 & 0 & 0 \\ \frac{82}{259} & \frac{116}{115} & \frac{567}{302} & \frac{149}{49} & 0 & 0 & 0 & 0 \\ 0 & 0 & 0 & 0 & \frac{239}{169} & \frac{239}{169} & \frac{239}{169} & \frac{239}{169} \\ 0 & 0 & 0 & 0 & \frac{94}{307} & \frac{203}{221} & \frac{173}{113} & \frac{688}{321} \\ 0 & 0 & 0 & 0 & \frac{41}{39} & \frac{183}{155} & \frac{95}{66} & \frac{53}{29} \\ 0 & 0 & 0 & 0 & \frac{82}{259} & \frac{116}{115} & \frac{567}{302} & \frac{149}{49} \end{bmatrix}. \quad (16)$$

2.1.3 Fibonacci wavelet operational matrices

In the sub-section, we now construct the operational matrices of Fibonacci wavelets in Equation (6), the authors Chen and Hsiao [22] introduce the strategy of operational matrices of integration as follows;

$$\int_0^z \Phi_{n,m}(\sigma)d\sigma = P\Phi_{n,m}(z), \quad (17)$$

Where P is the order of $2^{k-1}M \times 2^{k-1}M$, the Fibonacci wavelet operational matrix, by applying the power representation of Fibonacci wavelets and polynomials of the Equations (8) and (2), as well as binomial expansion of $(2^{k-1}z - n + 1)^{m-2i}$, then we get;

$$\psi_{n,m}(z) = \frac{2^{(k-1)/2}}{\sqrt{w_m}} \sum_{i=0}^{\lfloor m/2 \rfloor} \binom{m-i}{i} (2^{k-1}z - n + 1)^{m-2i} \chi_{\left[\frac{n-1}{2^{k-1}}, \frac{n}{2^{k-1}}\right]}(z),$$

$$\psi_{n,m}(z) = \frac{2^{(k-1)/2}}{\sqrt{w_m}} \sum_{i=0}^{\lfloor m/2 \rfloor} \sum_{j=0}^{m-2i} \binom{m-i}{i} 2^{kj-j} z^j (1-n)^{m-2i-j} \chi_{\left[\frac{n-1}{2^{k-1}}, \frac{n}{2^{k-1}}\right]}(z), \quad (18)$$

Integrate the above Equation (18), we have;

$$\int_0^z \psi_{n,m}(\sigma)d\sigma = \frac{2^{(k-1)/2}}{\sqrt{w_m}} \sum_{i=0}^{\lfloor m/2 \rfloor} \sum_{j=0}^{m-2i} \binom{m-i}{i} 2^{kj-j} z^j (1-n)^{m-2i-j} \chi_{\left[\frac{n-1}{2^{k-1}}, \frac{n}{2^{k-1}}\right]}(z)d\sigma,$$

$$= \frac{2^{(k-1)/2}}{\sqrt{w_m}} \sum_{i=0}^{\lfloor m/2 \rfloor} \sum_{j=0}^{m-2i} \binom{m-i}{i} 2^{kj-j} z^j (1-n)^{m-2i-j} R_j(z), \quad (19)$$

Where, $R_j(z) = \int_0^z \sigma^j \chi_{\left[\frac{n-1}{2^{k-1}}, \frac{n}{2^{k-1}}\right]}(\sigma)d\sigma,$

$$R_j(z) = \int_{n-1/2^{k-1}}^{z} \sigma^j \chi_{\left[\frac{n-1}{2^{k-1}}, \frac{n}{2^{k-1}}\right]}(z)d\sigma + \int_{n-1/2^{k-1}}^{n/2^{k-1}} \sigma^j \chi_{\left[\frac{n}{2^{k-1}}, 1\right]}(z)d\sigma,$$

$$0 \le j \le m - 2i. \quad (20)$$

In terms of Fibonacci wavelets, the function $R_j(z)$ may be represented as follows;

$$R_j(z) = \sum_{r=1}^{2^{k-1}} \sum_{s=0}^{M-1} \beta_{r,s} \psi_{r,s}(z), \quad (21)$$

As a result, Equation (19) has become;

$$\int_0^z \psi_{n,m}(\sigma)d\sigma = \sum_{r=1}^{2^{k-1}} \sum_{s=0}^{M-1} \Gamma_{r,s}^{n,m} \psi_{r,s}(z), \quad (22)$$

Where,

$$\Gamma_{r,s}^{n,m} = \frac{2^{(k-1)/2}}{\sqrt{w_m}} \sum_{i=0}^{\lfloor m/2 \rfloor} \sum_{j=0}^{m-2i} \binom{m-i}{i} 2^{kj-j} z^j (1-\eta)^{m-2i-j} \beta_{r,s}. \tag{23}$$

As a result, the operational integration matrix P for Fibonacci wavelets is as follows:

$$P = \begin{pmatrix} \Gamma_{1,0}^{1,0} & \Gamma_{1,1}^{1,0} & \cdots & \Gamma_{2^{k-1},M-1}^{1,0} \\ \Gamma_{1,0}^{1,1} & \Gamma_{1,1}^{1,1} & \cdots & \Gamma_{2^{k-1},M-1}^{1,1} \\ \vdots & \vdots & \vdots & \vdots \\ \Gamma_{1,0}^{2^{k-1},M-1} & \Gamma_{1,1}^{2^{k-1},M-1} & \cdots & \Gamma_{2^{k-1},M-1}^{2^{k-1},M-1} \end{pmatrix}. \tag{24}$$

In particular, if $k = 2$, $M = 4$, we may integrate Equation (8) using suitable collocation points provided in Equation (15), we obtain the coefficients of operational matrices as follows;

$$\int_0^z \psi_{1,0}(\sigma) d\sigma = \left(0, \frac{181}{627}, 0, 0, \frac{1}{2}, 0, 0, 0\right)^T \Phi_8(z),$$

$$\int_0^z \psi_{1,1}(\sigma) d\sigma = \left(-\frac{181}{627}, 0, \frac{155}{262}, 0, \frac{181}{418}, 0, 0, 0\right)^T \Phi_8(z),$$

$$\int_0^z \psi_{1,2}(\sigma) d\sigma = \left(0, \frac{5}{71}, 0, \frac{74}{539}, \frac{81}{166}, 0, 0, 0\right)^T \Phi_8(z),$$

$$\int_0^z \psi_{1,3}(\sigma) d\sigma = \left(-\frac{823}{2763}, \frac{-49}{209}, \frac{210}{521}, \frac{1}{4}, \frac{271}{488}, 0, 0, 0\right)^T \Phi_8(z),$$

$$\int_0^z \psi_{2,0}(\sigma) d\sigma = \left(0, 0, 0, 0, 0, \frac{181}{627}, 0, 0\right)^T \Phi_8(z),$$

$$\int_0^z \psi_{2,1}(\sigma) d\sigma = \left(0, 0, 0, 0, -\frac{181}{418}, 0, \frac{155}{262}, 0\right)^T \Phi_8(z),$$

$$\int_0^z \psi_{2,2}(\sigma) d\sigma = \left(0, 0, 0, 0, 0, \frac{5}{71}, 0, \frac{74}{539}\right)^T \Phi_8(z),$$

$$\int_0^z \psi_{2,3}(\sigma)d\sigma = \left(0,\ 0,\ 0,\ 0,\ -\frac{823}{2763},\ -\frac{49}{209},\ \frac{210}{521},\ \frac{1}{4}\right)^T \Phi_8(z).$$

Therefore, in the following Equation (17), we obtain the form:

$$\int_0^z \Phi_{8\times 1}(\sigma)d\sigma = P_{8\times 8}\Phi_8(z), \tag{25}$$

Where,

$$P_{8\times 8} = \begin{pmatrix} 0 & \frac{181}{627} & 0 & 0 & \frac{1}{2} & 0 & 0 & 0 \\ -\frac{181}{418} & 0 & \frac{155}{262} & 0 & \frac{181}{418} & 0 & 0 & 0 \\ 0 & \frac{5}{71} & 0 & \frac{74}{539} & \frac{81}{166} & 0 & 0 & 0 \\ -\frac{823}{2763} & -\frac{49}{209} & \frac{210}{521} & \frac{1}{4} & \frac{271}{488} & 0 & 0 & 0 \\ 0 & 0 & 0 & 0 & 0 & \frac{181}{627} & 0 & 0 \\ 0 & 0 & 0 & 0 & -\frac{181}{418} & 0 & \frac{155}{262} & 0 \\ 0 & 0 & 0 & 0 & 0 & \frac{5}{71} & 0 & \frac{74}{539} \\ 0 & 0 & 0 & 0 & -\frac{823}{2763} & -\frac{49}{209} & \frac{210}{521} & \frac{1}{4} \end{pmatrix}, \tag{26}$$

Similarly, we double integrate Equation (17), and we obtain Q an operational matrix as follows;

$$\int_0^z \int_0^z \Phi_{n,m}(\sigma)d\sigma = Q\Phi_{n,m}(z), \tag{27}$$

Where,

$$Q_{8\times 8} = \begin{pmatrix} -\frac{1}{8} & 0 & \frac{83}{486} & 0 & \frac{1}{8} & \frac{195}{1351} & 0 & 0 \\ 0 & -\frac{1}{12} & 0 & \frac{77}{948} & \frac{195}{2702} & \frac{1}{8} & 0 & 0 \\ -\frac{36}{509} & \frac{38}{1199} & \frac{23}{240} & \frac{15}{437} & \frac{19}{178} & \frac{141}{1001} & 0 & 0 \\ \frac{45}{1744} & -\frac{40}{351} & -\frac{24}{659} & \frac{139}{1200} & \frac{43}{505} & \frac{21}{524} & 0 & 0 \\ 0 & 0 & 0 & 0 & -\frac{1}{8} & 0 & \frac{83}{486} & 0 \\ 0 & 0 & 0 & 0 & 0 & -\frac{1}{12} & 0 & \frac{77}{948} \\ 0 & 0 & 0 & 0 & -\frac{39}{460} & -\frac{10}{483} & \frac{139}{1200} & \frac{9}{437} \\ 0 & 0 & 0 & 0 & \frac{2}{375} & -\frac{67}{684} & -\frac{3}{412} & \frac{23}{4=240} \end{pmatrix}. \quad (28)$$

2.2. Fibonacci wavelet operational matrix method of solution

Let us consider the general form of a second-order boundary value problem as;

$$\frac{d^2\theta_0}{dz^2} = f\left(z, \theta_0, \frac{d\theta_0}{dz}\right), \quad (29)$$

Following Shiralashetti et al. [18], we assume that;

$$\frac{d^2\theta_0(z)}{dz^2} = \sum_{i=1}^{2^{k-1}M} a_l \psi_l(z) = a^T \Phi(z), \quad (30)$$

Case (i) Suppose the given boundary conditions as;

$$\theta_0(0) = 0, \ \theta_0(1) = 1, \quad (31)$$

Integrating Equation (30) from 0 to z, we get;

$$\frac{d\theta_0(z)}{dz} = \frac{d\theta_0(0)}{dz} + \sum_{i=1}^{2^{k-1}M} a_l P_l(z) = \frac{d\theta_0(0)}{dz} + a^T P(z), \quad (32)$$

Again integrating Equation (32) from 0 to z and using the first boundary condition given in Equation (31), we get;

$$\theta_0(z) = z\,\frac{d\theta_0(0)}{dz} + \sum_{l=1}^{2^{k-1}M} a_l Q_l(z) = z\,\frac{d\theta_z(0)}{dz} + a^T Q(z), \tag{33}$$

From Equation (33), we can find $\frac{d\theta_0(0)}{dz}$, by using the second boundary condition given in Equation (31), we get;

$$\frac{d\theta_0(0)}{dz} = 1 - \sum_{i=1}^{2^{k-1}M} a_l C_l = 1 - a^T C, \tag{34}$$

Where, $C_i = \int_0^1 P_l(z)dz$, substituting $\theta_0(z)$, $\frac{d\theta_0(z)}{dz}$, and $\frac{d^2\theta_0(z)}{dz^2}$, in Equation (29), and using the collocation points in Equation (15), result in $2^{k-1}M \times 2^{k-1}M$ system of algebraic equations, these equations can be solved by using Newton's method with help of Matlab software to obtain the required Fibonacci wavelet coefficients a_l, $l = 1, 2, \ldots, 2^{k-1}M$. Finally substituting these obtained coefficients a_l's in Equation (33), to obtain the Fibonacci wavelet operational matrix method solution of the Equation (29) with (31).

Case (ii) Suppose the given boundary conditions as;

$$\frac{d\theta_0(0)}{dz} = 0,\ \theta_0(1) = 0, \tag{35}$$

Integrating Equation (30), from 0 to z, we get;

$$\frac{d\theta_0(z)}{dz} = 0,\ \theta_0(1) = 0, \tag{36}$$

Again integrating Equation (36) from 0 to z and using the first boundary condition from Equation (35), we get;

$$\theta_0(z) = \sum_{l=1}^{2^{k-1}M} a_l Q_l(z) + z\,\frac{d\theta_0(0)}{dz} + \theta_0(0) = a^T Q(z) + \theta_0(0), \tag{37}$$

From Equation (37), we can find $\theta_0(0)$ by using the second boundary condition from Equation (35), we get;

$$\theta_0(0) = -\sum_{i=1}^{2^{k-1}M} a_l C_l = -a^T C, \tag{38}$$

where, $C = \int_0^1 P_l(z)dz$, and a^T is the unknown Fibonacci wavelet coefficients, substituting $\theta_0(z)$, $\frac{d\theta_0(z)}{dz}$, and $\frac{d^2\theta_0(z)}{dz^2}$, in Equation (29), and by using the collocation points provided in Equation (15), it results in $2^{k-1}M \times 2^{k-1}M$ system of equations, these equations can be solved by using Newton's method to obtain the required Fibonacci wavelet coefficients a_l, $l = 1, 2, \ldots, 2^{k-1}M$. Finally substitute the obtained coefficients a_l's in Equation (37), to obtain the Fibonacci wavelet operational matrix method (FWOMM) of the solution of the equations (29) with (35).

Error Estimate. Absolute error can be obtained by using the relation [18] as;

$$e(z) = |\, \theta_0(z) - \theta_0^*(z) \,|, \; z \in [0, 1). \tag{38a}$$

Here, $\theta_0(z)$ and $\theta_0^*(z)$ are represented by exact solutions and numerical results of FWOMM.

2.3. Fibonacci wavelet operational matrix method of implementation

Test problem 1. Firstly, we consider the linear second-order boundary value problem [12] as;

$$\left.\begin{aligned} \frac{d^2\theta_0(z)}{dz^2} + e^{1/z}\frac{d\theta_0(z)}{dz} + \theta_0(z) - 6z - z^3 - 3z^2e^{1/z} = 0, \quad 0 < z < 1, \\ \theta_0(0) = 0, \qquad\qquad \theta_0(1) = 1. \end{aligned}\right\}, \tag{39}$$

Equation (39) has the exact solution $\theta_0(z) = z^3$. Using the method of the solution presented in section 2.2, obtaining the FWOMM of the solution as follows, substituting the Fibonacci wavelet approximations of $\frac{d^2\theta_0(z)}{dz^2}$, $\frac{d\theta_0(z)}{dz}$ and $\theta_0(z)$, in Equation (39) and using collocation points in

Equation (15), we obtained the system of equations as;

$$a^T[\Phi(z) + e^{1/z}(P(z) - C) + Q(z) - zC] + e^{1/z} - 5z - z^3 - 3z^2e^{1/z} = 0, \quad (40)$$

Solving the above system of equations by using the algebraic method and obtaining the required Fibonacci wavelet coefficients, if $k = 2$, $M = 4$, are $a_1 = -0.0000$, $a_2 = 1.2247$, $a_3 = 0.0000$, $a_4 = -0.0000$, $a_5 = 2.1213$, $a_6 = 1.2247$, $a_7 = 0.0000$, $a_8 = -0.0000$, Finally substituting these coefficients in equation (33), we get the FWOMM solution and which is presented in Table 1 and Figure 1, and also the comparison with the exact solution and Haar wavelet operational matrix method (HWOMM) of the solution.

Table1. Comparison of FWOMM solution with the exact solution and HWOMM solution of the test problem 1.

z	Exact solution	HWOMM solution $k = 2, M = 4.$	FWOMM solution $k = 2, M = 4.$	HWOMM Absolute Error $\lvert Exact - HWOMM \rvert$	FWOMM Absolute Error $\lvert Exact - FWOMM \rvert$
0.0	0.0000	0.0000	0.0000	0.0000	0.0000
0.1	0.0010	-0.0101	0.0010	0.0111	0.0000
0.2	0.0080	-0.0312	0.0312	0.0080	0.0000
0.3	0.0270	-0.0688	0.0270	0.0958	0.0000
0.4	0.0640	-0.1696	0.0640	0.2336	0.0000
0.5	0.1250	2.5126	0.1250	-2.3876	0.0000
0.6	0.2160	0.2275	0.2160	-0.0115	0.0000
0.7	0.3430	0.3081	0.3430	0.0349	0.0000
0.8	0.5120	0.4766	0.5120	0.0354	0.0000
0.9	0.7290	0.7072	0.7290	0.0218	0.0000

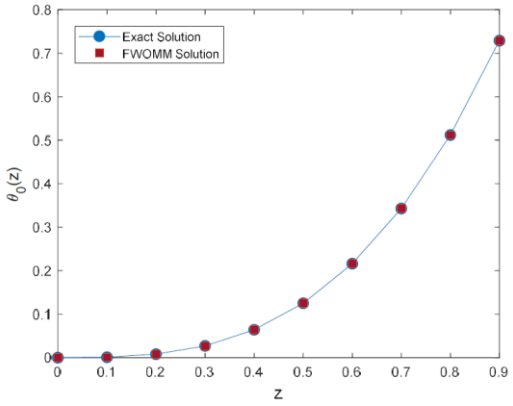

Figure 1. Solution of the FWOMM with the exact solution of the test problem 1.

Test problem 2. Next, consider the second-order nonlinear boundary value problem [13] as;

$$\left.\begin{array}{ll} \dfrac{d^2\theta_0(z)}{dz^2} + \theta_0^2(z) - z^4 - 2 = 0 & 0 < z < 1, \\ \theta_0(0) = 0 & \theta_0(1) = 1, \end{array}\right\}, \tag{41}$$

Equation (41) has the exact solution $\theta_0(z) = z^2$. Using the method of the solution presented in section 2.2, obtaining the FWOMM of the solution as follows, substituting the Fibonacci wavelet approximations of $\dfrac{d^2\theta_0(z)}{dz^2}$ and $\theta_0(z)$, in Equation (41) and using collocation points in Equation (15), we obtained the nonlinear algebraic system of equations

$$\sum_{i=1}^{2^{k-1}M} a_i(\Phi_i(z)) + \left[\sum_{i=1}^{2^{k-1}M} a_i(p_i(z) - zC_l) + z\right]^2 - z^4 - 2 = a^T\Phi(z)$$

$$+ [a^T(P(z) - zC) + z]^2 - z^4 - 2 = 0. \tag{42}$$

Solving the above system of equations by using Newton's method and obtaining the required Fibonacci wavelet coefficients, if $k = 2$, $M = 4$, are $a_l = 1.4142$, $a_2 = 0.0000$, $a_3 = 0.0000$, $a_4 = -0.0000$, $a_5 = 1.4142$,

$a_6 = -0.0000$, $a_7 = 0.0000$, $a_8 = -0.0000$, Finally substituting these coefficients in Equation (33), we get the FWOMM solution and it is presented in Table 2 and Figure 2 in comparison with the exact solution and HWOMM of the solution.

Table 2. Comparison of FWOMM solution with the exact solution and HWOMM solution of the test problem 2.

z	Exact solution	HWOMM solution $k = 2,\ M = 4.$	FWOMM solution $k = 2,\ M = 4.$	HWOMM Absolute Error $\lvert Exact - HWOMM \rvert$	FWOMM Absolute Error $\lvert Exact - FWOMM \rvert$
0.0	0.0000	0.0000	0.0000	0.0000	0.0000
0.1	0.0100	0.0100	0.0100	0.0000	0.0000
0.2	0.0400	0.0400	0.0400	0.0000	0.0000
0.3	0.0900	0.0900	0.0900	0.0000	0.0000
0.4	0.1600	0.1600	0.1600	0.0000	0.0000
0.5	0.2500	0.2500	0.2500	0.0000	0.0000
0.6	0.3600	0.3600	0.3600	0.0000	0.0000
0.7	0.4900	0.4900	0.4900	0.0000	0.0000
0.8	0.6400	0.6400	0.6400	0.0000	0.0000
0.9	0.8100	0.8100	0.8100	0.0000	0.0000

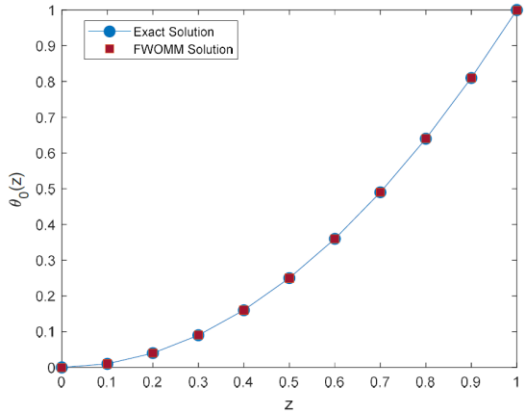

Figure 2. Numerical solution of FWOMM with the exact solution of the test problem 2.

Heat transfer Problem 3. The mathematical formulation of the

problem: we now introduce a simple pseudo-homogeneous model for understanding convection driven by an exothermic process. The normal continuity and momentum balancing assumptions are required. Assuming the Boussinesq approximation holds if Darcy's law is true. Because density differences are minor, they solely affect the body force term. Assuming a high Prandtl number for the porous medium. That is, the momentum balance's acceleration terms are minimal. With the stated assumptions, the governing equations

$$\nabla \cdot u = 0, \tag{43}$$

$$\nabla p = -\left(\frac{\mu_0}{k}\right)u - \rho_f[1 - b(T - T_0)]ge_z, \tag{44}$$

$$\rho_m C_{pm} \frac{\partial T}{\partial t} + \rho_f C_{pf} u \cdot \nabla T = k_{eff}\nabla^2 T + (-\Delta H)r, \tag{45}$$

$$\in \frac{\partial c_{Af}}{\partial t} + u \cdot \nabla c_{Af} = D_{eff}\nabla^2 c_{Af} - r, \tag{46}$$

Where the first-order reaction rate is given by;

$$r = k(T)c_{Af}, \tag{47}$$

$$k(T) = k_0 \exp(-E/RT) = k(T_0)\exp\left(\frac{E}{RT_0} + \frac{-E}{RT}\right), \tag{48}$$

Here, parameters p, T, c_{Af} are indicates pressure, temperature, and concentration of the fluid u represents superficial, $\in$ indicate the porosity or fractional profile of the fluid phase, b is the fluid's density coefficient at room temperature T_0, and the unit vector e_z is vertically upward oriented. Here, $\rho_m C_{pm} = \in \rho_f C_{pf} + (1- \in)\rho_s C_{ps}$, is the specific heat capacity of the bed per unit volume and $\rho_f C_{pm}, \rho_s C_{ps}$ are the fluid's and solid's respective heat capacities per cubic meter. The D_{eff} and e_{eff} are denoted by effective thermal diffusivity and conductivity of the bed, k which is denoted by the permeability of the porous medium. Equation (45) shows the reaction terms as a source while Equation (46) shows them as a sink Equation (46). The heat of the reaction as a mole of extent is represented by the constant $(-\Delta H)$, and

the reaction rate per unit volume is represented by r. The inter-phase concentration and temperature gradients are omitted while constructing the continuity Equations (45) and (46). The system is described by a single concentration and temperature. For vanish small particle heat and mass Damkohler numbers, this pseudo-homogeneous description is valid, which is represented as [6],

$$Da_{ph} = \frac{k(T_0)P_{f0}c_{f0}d_p}{h_c}, \tag{49}$$

$$Da_{pm} = \frac{k(T_0)d_p}{k_c}, \tag{50}$$

Where, d_p is the size of the particle, k_c and h_c are the coefficients of local heat and mass transfer. The density change as concentration is disregarded in Equation (44). If the reactions do not entail a variation in the number of moles, this model is appropriate. The situation of a rectangular shape box $(0 < z' < H, 0 < x' < L)$ is taken into consideration. The following corresponding boundary criteria apply to the box's bottoms and sidewalls [6].

$$\left.\begin{aligned} u \cdot e_n &= 0, \\ \nabla T \cdot e_n &= 0, \\ \nabla c_{Af} \cdot e_n &= 0, \end{aligned}\right\}, \tag{51}$$

The unit external normal is denoted by the letter e_n. We will get the simplest Dirichlet boundary conditions by opening the box to the atmosphere at the top. At $z' = H$, we have;

$$\left.\begin{aligned} \rho &= p_\alpha, \\ T &= T_0, \\ c_{Af} &= c_{Af0}, \end{aligned}\right\}, \tag{52}$$

The following values are defined to translate the system of equations into a non-dimensional form as follows;

$$\left.\begin{aligned} z = \frac{z'}{H},\ \theta = \gamma\frac{T-T_0}{T_0},\ x = \frac{x'}{L},\ \tau = \frac{u^*t}{\sigma H},\\ x = \frac{c_{Af}}{C_{Af0}},\ \lambda_m = \frac{k_{eff}}{\rho_f C_{pf}},\ \Pi = \frac{k(p-p_a)}{\mu\lambda_m},\ u^* = \frac{\lambda_m}{H},\\ \nu = \frac{u}{\sigma u^*},\ \sigma = \frac{\in \rho_f C_{pf}}{\rho_m C_{pm}},\ \alpha = \frac{L}{H},\ L_e = \frac{\lambda_m}{D_{eff}},\\ Ra = \frac{\rho_f^2 C_{pf} g H b T_0 k}{\gamma\mu k_{eff}},\ \varphi^2 = \frac{k(T_0)H^2}{\lambda_m}, \end{aligned}\right\}, \tag{53}$$

Here, z and x are the vertical and horizontal non-dimensional coordinate axes, correspondingly, and τ denotes the non-dimensional time. The mainly represents three nondimensional parameters such as temperature profile θ, pressure gradient Π, and concentration term c, with we are also introduced the velocity profile term u^* and we applying dimensionless velocity u. The stream function formula is introduced in the article [5];

$$\left.\begin{aligned} \nu_x &= \alpha\times\frac{\partial\psi}{\partial z},\\ \nu_z &= -\frac{\partial\psi}{\partial x}, \end{aligned}\right\}, \tag{54}$$

We obtain the equations, substituting Equations (53) and (54), into the Equations (43-52);

$$\frac{\partial^2\psi}{\partial x^2} + \alpha^2\times\frac{\partial^2\psi}{\partial z^2} + Ra\times\frac{\partial\theta}{\partial x} = 0, \tag{55}$$

$$\frac{\partial\theta}{\partial\tau} = \left(\frac{1}{\alpha^2}\frac{\partial^2\theta}{\partial x^2} + \frac{\partial^2\theta}{\partial z^2}\right) - \left(\frac{\partial\theta}{\partial x}\frac{\partial\psi}{\partial z} - \frac{\partial\psi}{\partial x}\frac{\partial\theta}{\partial z}\right) + B\phi^2 c\exp\left(\frac{\theta\gamma}{\theta+\gamma}\right), \tag{56}$$

$$Le\sigma\frac{\partial c}{\partial\tau} = \left(\frac{1}{\alpha^2}\frac{\partial^2 c}{\partial x^2} + \frac{\partial^2 c}{\partial z^2}\right) - Le\left(\frac{\partial c}{\partial x}\frac{\partial\psi}{\partial z} - \frac{\partial\psi}{\partial x}\frac{\partial c}{\partial z}\right) - \phi^2 c\exp\left(\frac{\theta\gamma}{\theta+\gamma}\right), \tag{57}$$

depending on;

$$\left.\begin{aligned} \frac{\partial c}{\partial x} = 0, \frac{\partial\theta}{\partial x} = 0, at\ x = 0,1,\\ \frac{\partial c}{\partial z} = 0, \frac{\partial\theta}{\partial x} = 0, at\ z = 0,\\ \theta = 0, \frac{\partial\psi}{\partial z} = 0, at\ z = 1, \end{aligned}\right\}. \tag{58}$$

Here, Ra represent Rayleigh number; this is indeed the ratio of heat diffusion characteristic time to natural convection characteristic time. The thermal Thiele parameter ϕ^2 is the ratio of diffusion to reaction characteristic time. In the absence of natural free convection, the value B is the maximal temperature that can be reached. The γ nondimensional activation energy is a metric for the rate of a reaction constant's temperature sensitivity. The proportion of the heat to mass diffusivity is known as the Lewis number Le. The variable σ is the aspect ratio of the box and the parameter σ is the ratio of volume heat capacities. Natural convection is considered to be completely absent $\psi = 0$ in the base case, and the result is only influenced by reaction and diffusion. Assume that the state parameters θ, c depending on the vertical coordinate based on the medial boundary conditions. According to the assumption, the mathematical equations describe the state of conductivity (diffusion).

$$\frac{\partial \theta}{\partial \tau} = \frac{\partial^2 \theta}{\partial z^2} + \left(B\phi^2 c \exp\left(\frac{\theta\gamma}{\theta\gamma} \right) \right), \tag{59}$$

$$Le\sigma \frac{\partial c}{\partial \tau} = \frac{\partial^2 c}{\partial z^2} - \left(\phi^2 c \exp\left(\frac{\theta\gamma}{\theta\gamma} \right) \right), \tag{60}$$

depending on;

$$\left.\begin{array}{c} \frac{dc}{dz} = 0, \frac{d\theta}{dz} = 0 \text{ at } z = 0, \\ c = 1, \theta = 0, \text{ at } z = 1, \end{array}\right\}. \tag{61}$$

Equations (59-61) can be integrated with a steady-state situation to;

$$c_0(z) = 1 - \frac{\theta_0(z)}{B}, \tag{62}$$

Here, the steady-state concentration and temperature profiles are c_0 and θ_0, correspondingly. The two-point boundary value problems for the diffusion (conduction) state's temperature profile are given by inserting this in the constant energy balance, Equation (59). We obtained as;

$$\frac{d^2\theta_0}{dz^2} + \phi^2 B\left(1 - \frac{\theta_0}{B}\right) \exp\left(\frac{\theta_0 \gamma}{\theta_0 + \gamma} \right) = 0, \tag{63}$$

$$\left.\begin{aligned} \frac{d\theta_0}{dz}(z) = 0, \quad & \text{at } z = 0, \\ \theta_0(z) = 0, \quad & \text{at } z = 1, \end{aligned}\right\}. \tag{64}$$

Where, B is the variable of maximum achievable temperature in the absence of natural free convection. The ϕ^2 represents the ratio of the characteristic typical time of diffusion of the heat generator γ is the non-dimension activation energy. Equation (63) becomes Equation (65) if the source of heat remains constant $(\gamma = 0)$.

$$\frac{d^2\theta_0}{dz^2} + \phi^2 B\left(1 - \frac{\theta_0}{B}\right) = 0, \tag{65}$$

With boundary conditions are;

$$\left.\begin{aligned} \frac{d\theta_0}{dz}(z) = 0, \quad & \text{at } z = 0, \\ \theta_0(z) = 0, \quad & \text{at } z = 1, \end{aligned}\right\}. \tag{66}$$

Case I. FWOMM solution of the Equations (65) with (66) is as follows: We now consider the two-point boundary value problem for the constant heat source $(\gamma = 0)$ in the porous medium, the temperature profile $\theta_0(z)$, in Equation (63). We get a constant heat source Equation (65).

Using the method of the solution presented in section 2.2, obtaining the FWOMM of solution as follows, substituting the Fibonacci wavelet approximations of $\frac{d^2\theta_0(z)}{dz^2}$ and $\theta_0(z)$, in Equation (65) and using collocation points in Equation (15), we obtained the system of equations as;

$$\sum_{i=1}^{2^{k-1}M} a_i(\Phi_i(z) - \varphi^2 Q_i(z) + \varphi^2 C_i) + B\varphi^2 = a^T(\Phi(z) - \varphi^2 Q(z) + \varphi^2 C) + B\varphi^2 = 0. \tag{68}$$

Solving the above system of equations by using the Newton's method and obtaining the required Fibonacci wavelet coefficients for $k = 2$, $M = 4$, are $a_1 = -3.1583$, $a_2 = 0.0046$, $a_3 = -0.2832$, $a_4 = -0.0050$, $a_5 = -3.3560$,

$a_6 = -0.2341$, $a_7 = -0.3041$, $a_8 = -0.0133$, finally substituting these coefficients in Equation (37), we get the FWOMM solution and it is presented in Table 3 and Figures 3 and 4 in comparison with the FDM (Finite Difference Method) solution and Haar wavelet operational matrix method (HWOMM) of solution.

Table 3. Comparison of FWOMM solution $\theta_0(z)$ with the FDM solution and HWOMM solution of the Equations (65) with (66) for $\varphi^2 = 0.5$, $B = 12$.

z	Exact solution	HWOMM solution $k = 2$, $M = 4$.	FWOMM solution $k = 2$, $M = 4$.	HWOMM Absolute Error $\lvert Exact - HWOMM \rvert$	FWOMM Absolute Error $\lvert Exact - FWOMM \rvert$
0.0	2.4804	2.4004	2.4804	0.0800	0.0000
0.1	2.4566	2.3798	2.4566	0.0768	0.0000
0.2	2.3851	2.3217	2.3851	0.0634	0.0000
0.3	2.2655	2.2105	2.2654	0.0550	0.0001
0.4	2.0972	2.0611	2.0971	0.0361	0.0001
0.5	1.8793	1.8606	1.8781	0.0187	0.0012
0.6	1.6109	1.5985	1.6099	0.0124	0.0010
0.7	1.2904	1.2881	1.2897	0.0023	0.0007
0.8	0.9164	0.9161	0.9160	0.0003	0.0004
0.9	0.4870	0.4884	0.4869	0.0014	0.0001

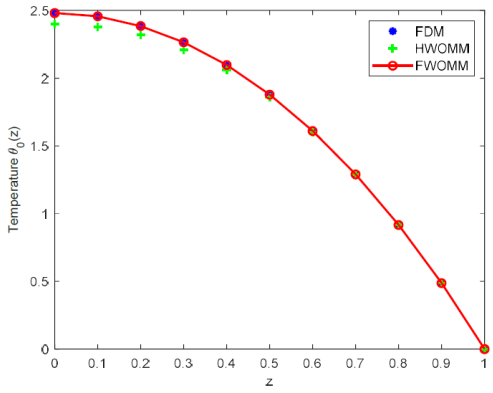

Figure 3. Solutions of FWOMM with the FDM and HWOMM solution of the Equations (65) with (66) for $\varphi^2 = 0.5$, $B = 12$.

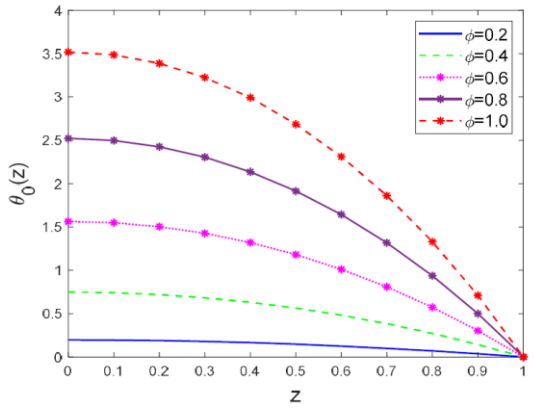

Figure 4. Effect of FWOMM solution $\theta_0(z)$ of the Equations (65) with (66) for altered values of ϕ with a constant value of $B = 10$.

Case II. FWOMM solution of the Equations (63) with (64) is as follows; Next, we consider the two-point nonlinear boundary value problem for the Conduction state's temperature profile $\theta_0(z)$ in the presence of a porous medium. Using the method of the solution presented in section 2.2, obtaining the FWOMM of solution as follows, substituting the Fibonacci wavelet approximations of $\frac{d^2\theta_0(z)}{dz^2}$ and $\theta_0(z)$, in Equation (63) and using collocation points in Equation (15), we obtained the nonlinear system of equations as;

$$a^T F(z) + B\phi^2 \exp\left(\left[\frac{\gamma a^T (Q(z) - C)}{\gamma + a^T (Q(z) - C)}\right]\right)$$

$$-\phi^2 a^T (Q(z) - C) \exp\left(\left[\frac{\gamma a^T (Q(z) - C)}{\gamma + a^T (Q(z) - C)}\right]\right) = 0. \tag{69}$$

Solving the above system of equations by using the Newton's method and obtaining the required Fibonacci wavelet coefficients if $k = 2$, $M = 4$, $\lambda = 1$, are $a_1 = -5.2428$, $a_2 = -0.1609$, $a_3 = -1.0496$, $a_4 = 0.1788$, $a_5 = -5.7931$, $a_6 = -3.4545$, $a_7 = -1.0594$, $a_8 = 2.8724$, finally substituting these coefficients in equation (37), we get the FWOMM solution and it is presented in Table 4 and Figures 5 and 6 in comparison with the HWOMM of the solution.

Table 4. Comparison of FWOMM solution $\theta_0(0)$ with the HWOMM solution of the Equations (63) with (64) for $\varphi^2 = 0.5$, $B = 12$, $\lambda = 1$.

z	FWOMM solution $k = 2$, $M = 4$.	
0.0	4.3246	4.5053
0.1	4.2903	4.4617
0.2	4.1975	4.3338
0.3	4.0043	4.1195
0.4	3.7486	3.8170
0.5	3.3932	3.4381
0.6	2.9168	2.9418
0.7	2.3427	2.3499
0.8	1.6579	1.6610
0.9	0.8688	0.8708

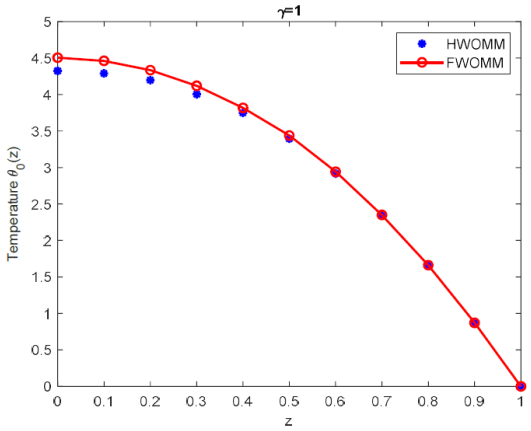

Figure 5. Numerical solution of FWOMM with the HWOMM solution of the Equations (63) with (64) for $\varphi^2 = 0.5$, $B = 12$, $\gamma = 1$.

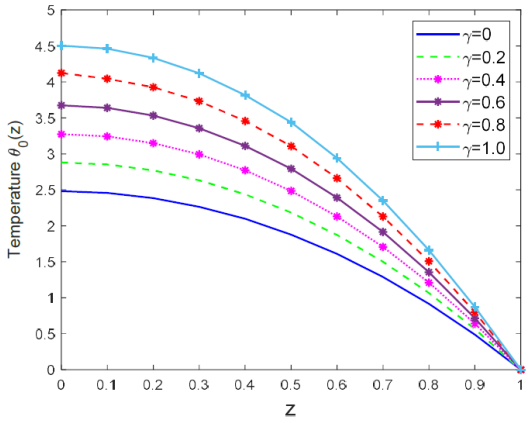

Figure 6. Effect of FWOMM solution $\theta_0(z)$ of the Equations (63) with (64) for altered values of ϕ with $\varphi^2 = 0.5$, $B = 12$.

3. Results and Discussions

The study presents, that the computations were performed numerically to analyze the physical boundary value problem for different values of parameters that explain the detail, and the solutions are shown in terms of tables and graphs. Our aim here is to contribute to the qualitative behavior and physical attitudes of the problem. The differential equations (39), (41), (63), and (65) with corresponding boundary conditions are thoroughly examined by using the Fibonacci wavelet operational matrix method (FWOMM).

We observed that Tables 1 and 2 show the comparison of FWOMM solutions with the exact, and HWOMM solutions. Figures 1 and 2 show the comparison of FWOMM solutions with the exact solutions. The FWOMM solutions are more accurate than the HWOMM solutions, and in excellent agreement with the exact solutions.

We have considered the highest temperature in the absence of natural convection B and the ratio of conduction to heat generation ϕ^2 the non-dimensional activation energy γ because the heat source is constant. We observed that Table 3, shows the comparisons of the steady-state temperature profile $\theta_0(z)$ of the FWOMM, Finite difference method (FDM), and HWOMM

for the parameters $k = 2$, $M = 4$. $\varphi^2 = 0.5$, $B = 12$, the comparisons of FWOMM solutions are more accurate results as compared to the HWOMM solutions are represented in Table 3. Figure 3 shows a graphical depiction of the results using the finite difference methodology [5], HWOMM, and FWOMM with good agreement. We observed that FWOMM provides a more accurate solution than the classical HWOMM. Displayed Figure 4 shows the influence of various variations of ϕ with a constant value B on the temperature profile $\theta_0(z)$. When the Heat generation parameter ϕ is increased, also increases the temperature profile $\theta_0(z)$ with a constant value B. Also, we have considered the conduction state's temperature profile $\theta_0(z)$ in the presence of a porous medium. In Equation (63) the nondimensional activation energy γ is considered. Displayed Table 4, shows the comparison of the FWOMM with the HWOMM solutions. We see the Table 4, that a comparison of FWOMM solutions is more accurate than the HWOMM solutions. And also observed the Figure 5, comparisons of the Fibonacci solutions are more accurate as compared to the Haar results. Displayed Figure 6 shows the influence of various variations of ϕ with a constant value $\phi^2 = 0.5$, $B = 12$, of the temperature profile $\theta_0(z)$. When the non-dimensional activation energy γ is increased, also increases the temperature profile $\theta_0(z)$ with a constant value of $\varphi^2 = 0.5$, $B = 12$. We observed in Tables and Graphs, that the numerical outcomes obtained by using FWOMM are in very excellent agreement with the obtained Haar wavelet operational matrix method (HWOMM) results. On the contrary, the typical Haar wavelets technique produces a good solution, but FWOMM produces excellent solutions as compared to HWOMM. As a result, the FWOMM solutions are easier to implement than the HWOMM results.

4. Conclusions

In this paper, we discuss an arithmetical scheme to solve boundary value problems. Using the operational matrices based on the Fibonacci wavelets, the characteristic nonlinear boundary value problems can be transformed into a set of algebraic equations. Then we can govern the unidentified coefficients. To check the efficiency of the proposed method, the second-order

linear and nonlinear boundary value problem having the exact solution is considered test problems 1 and 2. Consequences display the Fibonacci wavelet operational matrix method is an appropriate and vigorous scheme in discovery resolutions to boundary value problems. Further, we have described an exothermic reaction model in the presence of porous media with a constant heat source. The governing Equations (63) and (65) of the problems with proper boundary conditions are reduced into the characteristic nonlinear boundary value problems by applied similarity transformations. These problems are solved by using the Fibonacci wavelet operational matrix method and the results are presented in terms of tables and graphs. The efficiency of the proposed method is confirmed by determining the comparison of resolutions which are demonstrated in Tables and Figures. Figures 4 and 6, demonstrate the influence of various variations with constant values parameters on the temperature profile. This shows the comparison of steady-state temperature profiles for the exact solution, Haar wavelet operational matrix method of solution, and efficiency of the proposed Fibonacci wavelet operational matrix method of solution.

Acknowledgement

We thank UGC-SAP DRS-III for 2016-2021: F.510/3/DRS-III / 2016(SAP-I) Dated: 29th Feb. 2016. And this work is supported by Karnatak University, Dharwad (KUD), Karnataka India through a University Research Studentship (URS) during the year 2018-2021: KU.40 (SC/ST) sch/URS/2020-21/44/544, dated 12/12/2020.

References

[1] J. L. Beck, Convection in a box of porous material saturated with fluid, The Physics of Fluids 15(8) (1972), 1377-1383. https://doi.org/10.1063/1.1694096

[2] A. Donald, Nield and A. Adrian Bejan, Convection in Porous Media, Chapter 5, Springer International Publishing, 5th edition, 2017. http://library.lol/main/2F8F5BDF933FC0BA87F849C58065BFBA.

[3] S. H. Davis, Convection in a box: Linear theory, Journal of Fluid Mechanics 30(3) (1967), 465-478. DOI: https://doi.org/10.1017/S0022112067001545

[4] Z. Gershuni and E. M. Zhukovitskii, Convective stability of incompressible fluids, Israel Program for Scientific Translations 1976. https://agris.fao.org/agris-search/search.do?recordID=US201300535712

[5] S. Subramanian and V. Balakotaiah, Convective instabilities induced by exothermic reactions occurring in a porous medium, Physics Fluids 6(9) (1994), 2907-2922. https://doi.org/10.1063/1.868119

[6] N. Pochai and J. Jaisaardsuetrong, A numerical treatment of an exothermic reactions model with constant heat source in a porous medium using finite difference method, Advanced Studies in Biology 4(6) (2012), 287-296. http://www.m-hikari.com/asb/asb2012/asb5-8-2012/pochaiASB5-8-2012.pdf

[7] H. Viljoen and V. Hlavacek, Chemically driven convection in aporous medium, AIChE Journal 33(8) (1987), 1344-1350. https://doi.org/10.1002/aic.690330811

[8] H. J. Viljoen, J. E. Gatica and H. Vladimir, Bifurcation analysis of chemically driven convection. Chemical Engineering Science 45(2) (1990), 503-517. https://doi.org/10.1016/0009-2509(90)87037-S

[9] K. Nandakumar and H. J. Weinitschke, A bifurcation study of chemically driven convection in a porous medium, Chemical Engineering Science 47(15-16) (1992), 4107-4120. https://doi.org/10.1016/0009-2509(92)85161-4

[10] F. Mabood and N. Pochai, Optimal homotopy asymptotic solution for exothermic reactions model with constant heat source in a porous medium, Advances in Mathematical Physics 2015. https://doi.org/10.1155/2015/825683

[11] R. P. Sharma, M. Jain and D. Kumar, Analytical solution of exothermic reactions model with constant heat source and porous medium, Proceedings of the National Academy of Sciences, India Section A: Physical Sciences 90(2) (2020), 239-243. https://doi.org/10.1007/s40010-018-0562-y

[12] A. K. Nasab, A. Kılıçman, E. Babolian and Z. P. Atabakan, Wavelet analysis method for solving linear and nonlinear singular boundary value problems, Applied Mathematical Modelling 37(8) (2013), 5876-5886. https://doi.org/10.1016/j.apm.2012.12.001

[13] A. J. Mohamad, Solving second order non-linear boundary value problems by four numerical methods, Engineering Technology Journal 28(2) (2010), 369-381.

[14] S. C. Shiralashetti and S. I. Hanaji, Hermite wavelet-based numerical method for the solution of two parameters singularly perturbed non-linear Benjamina-Bona-Mohany equation, Scientific African 2021; 12:e00770. https://doi.org/10.1016/j.sciaf.2021.e00770

[15] S. C. Shiralashetti and P. Badiger, Chebyshev wavelets approach for the squeeze film lubrication of long porous journal bearings with couple stress fluids, Malaya Journal of Matematik S (1) (2020), 138-143. https://doi.org/10.26637/MJM0S20/0026

[16] S. C. Shiralashetti, and E. Harishkumar, Haar wavelet matrices for the numerical solution of a system of ordinary differential equations, Malaya Journal of Matematik, S (1) (2020), 144-147. https://doi.org/10.26637/MJM0S20/0027

[17] S. C. Shiralashetti, L. M. Angadi and A. B. Deshi, Numerical solution of some class of nonlinear partial differential equations using wavelet-based full approximation scheme, International Journal of Computational Methods 17(6) (2020), 1950015. https://doi.org/10.1142/S0219876219500154

[18] S. C. Shiralashetti, L. M. Angadi and S. Kumbinarasaiah, Laguerre wavelet-Galerkin method for the numerical solution of one dimensional partial differential equations, International Journal of Mathematics And its Applications 6(1-E) (2018), 939-949. http://ijmaa.in/

[19] F. A. Shah, M. Irfan, K. S. Nisar, R. T. Matoog and E. E. Mahmoud, Fibonacci wavelet method for solving time-fractional telegraph equations with Dirichlet boundary conditions, Results in Physics 24(1) (2021), 104123. https://doi.org/10.1016/j.rinp.2021.104123

[20] S. Sabermahani, Y. Ordokhani and S. A. Yousefi, Fibonacci wavelets and their applications for solving two classes of time-varying delay problems, Optimal Control Applications and Methods 41(2) (2020), 395-416. https://doi.org/10.1002/oca.2549

[21] M. Cakmak, Fibonacci operational matrix algorithm for solving differential equations of Lane-Emden type, Sakarya University Journal of Science 23(3) (2019), 478-485. https://doi.org/10.16984/saufenbilder.344991

[22] C. F. Chen and C. Hsiao, Haar wavelet method for solving lumped and distributed parameter systems, IEE Proc-Control Theory Applications 144(1) (1997), 87-94. doi.org/10.1049/ip-cta:19970702.